Available online at www.sciencedirect.com
SCIENCE DIRECT®
Chemical Physics Letters 415 (2005) 291–295
CHEMICAL PHYSICS LETTERS
www.elsevier.com/locate/cplett

Isotope effects in the ultrafast photodissociation of acetone 3s Rydberg state excited at 195 nm

Wei-Kan Chen, Jr-Wei Ho, Po-Yuan Cheng *

Department of Chemistry, National Tsing Hua University, 101 Sec.2 Kuang Fu Rd., Hsinchu 30013, Taiwan, ROC

Received 18 May 2005; in final form 4 September 2005
Available online 28 September 2005

Abstract

The deuterium isotope effect in the photodissociation of acetone S_2 state was studied using femtosecond pump–probe ionization spectroscopy. The transients obtained for both isotopomers can be well described by the same mechanism in which the primary dissociation occurs on the S_1 surface. Substantial isotope effects were observed in every stage of the reaction. Our results indicted that upon full deuteration the initial-state decay from S_2 to S_1 slows down by a factor of three, the subsequent adiabatic dissociation on the S_1 surface slows down by a factor of four, and the secondary dissociation slows down by a factor of ~1.6.

1. Introduction

Photodissociation of acetone in the ultraviolet region has been extensively studied for decades [1–20]. At sufficiently high excitation energies the two equivalent α-CC bonds can both break [6,8,9], producing a CO and two CH_3 radicals. In the case of excitation to the low-energy regions of the $S_1(n,\pi^*)$ state, previous studies have concluded that the primary α-CC dissociation occurs on the first triplet-state surface following a fast $S_1 \rightarrow T_1$ intersystem crossing (ISC) step [7,9,21]. The resulting hot acetyl radical then undergoes a secondary dissociation to break another α-CC bond, provided that its internal energy is high enough [9]. It has been commonly assumed [5,8,9,11,12,19] that excitation to the acetone higher states, for example the $S_2(n,3s)$ Rydberg state, follows a similar pathway; i.e., fast internal conversion (IC) and ISC processes rapidly bring the molecule to the first triplet state where the dissociation takes place by overcoming a low barrier. However, this notion has been challenged by recent theoretical [15,16] and experimental studies [18,22,23]. Based on the theoretical insight that the barrier to α-CC dissociation leading to linear $CH_3CO(\tilde{A})$ is low on the S_1 surface [15,16], a different mechanism assuming the primary dissociation occurs on the S_1 surface following the $S_2 \rightarrow S_1$ internal conversion has been proposed (see Scheme 1) [15,16]. For the sake of convenience, this newly proposed mechanism is referred to as the 'S_1 dissociation (S_1D) mechanism,' and the commonly adopted one is referred to as the 'T_1 dissociation (T_1D) mechanism.'

We have reported our recent studies on the photodissociation of acetone S_2 state with the focus on differentiation between the two mechanisms (S_1D vs. T_1D) [18,22,23]. We measured the temporal evolutions of the initial state, acetyl intermediates and the methyl products simultaneously using femtosecond (fs) mass-selected pump–probe multiphoton ionization (MPI) spectroscopy [22]. We also employed fs time-resolved photofragment translational spectroscopy (TR-PTS) to measure the temporal evolution of the CH_3-product kinetic-energy distributions and resolved the primary and secondary components [23]. Both techniques yielded complementary and consistent results that support the validity of the S_1D mechanism. Our conclusion is summarized in Scheme 1 as a kinetic model. Briefly, upon photoexcitation of acetone at 195 nm the initially-excited S_2 state first undergoes a relatively slow IC (~4 ps) to the S_1 state. The internally converted S_1 state

* Corresponding author. Fax: +3 571 1082.
E-mail address: pycheng@mx.nthu.edu.tw (P.-Y. Cheng).

0009-2614/$ - see front matter © 2005 Elsevier B.V. All rights reserved.
doi:10.1016/j.cplett.2005.09.021

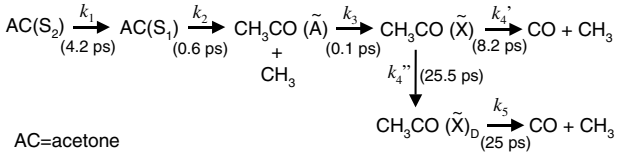

Scheme 1.

possesses an enormous amount of 250 kJ/mol vibrational energy and rapidly undergoes an adiabatic dissociation along the α-CC coordinate in about 0.6 ps to produce a methyl radical and an electronically excited acetyl radical, $CH_3CO(A)$ The latter internally converts to its ground state, $CH_3CO(\tilde{X})$, in about 100 fs, producing a hot acetyl ground state that subsequently undergoes a secondary dissociation to produce another methyl radical and a carbon monoxide [22,23].

The secondary dissociation of the hot acetyl radical was shown to be very complex in our studies [22,23]. We proposed that a rather large fraction of the vibrational energy in $CH_3CO(\tilde{X})$ is initially localized in the CCO bending mode due to the great geometrical change along this coordinate during the primary dissociation and the ultrafast $CH_3CO\tilde{A} \rightarrow \tilde{X}$ IC. The entire secondary dissociation can be approximately described by two discernable stages [22]. In the first stage, a large portion of the energy is trapped in the bending coordinate due to a very slow CCO bending-energy dissipation, and those dissociate in this stage (~6 ps) are those with higher internal energy in the entire distribution of the acetyl ensemble. This stage is referred to as the *fast secondary dissociation*. Those left behind after the concurrent steps of the fast secondary dissociation and CCO bending relaxation are not only more bend-relaxed but also contain less average vibrational energy due to the evaporative cooling effect. They thus dissociate more slowly with a time constant of about 25 ps. This second stage of the reaction is referred to as the *slow secondary dissociation*.

In this letter, we extend our previous works [22,23] to examine the isotope effects in the title reaction. The purpose is to seek for further supports to the validity of the S_1D mechanism and additional insights by comparing the photodissociation dynamics of the fully deuterated acetone-d_6 and the undeuterated acetone-h_6.

2. Experimental

The experimental set up and procedures used in this work are essentially the same as those described in our previous works [22,23]. The fs laser system consists of a self-mode-locked Ti:sapphire laser, a 1-kHz chirped-pulse regenerative amplifier (CPA) and a five-pass optical parametric generator/amplifier. For acetone-h_6 the oscillator/amplifier output was tuned to 780 nm; while for acetone-d_6 the output was tuned to 778 nm. The CPA output was split into two parts by a beam splitter. The major portion (~80%) of the beam was used to pump the optical parametric amplifier, whose signal output at ~1334 nm (1336 nm) was subsequently frequency-doubled twice to produce probe pulses at ~333.5 nm (334.0 nm) for the $2+1$ REMPI detection of CH_3 (CD_3) radicals [24]. The same probe pulses were also used to probe the initial state and acetyl intermediate.

The remaining portion of the CPA output (~20%) was first directed through a retroreflector mounted on a computer-controlled translation stage and was then sent into a harmonic generator to produce the fourth harmonic at ~195 nm (194.5 nm), which was used as the pump to excite acetone-h_6 (acetone-d_6) to the S_2 origin region [20]. The pump and probe beams were colinearly recombined via a dichroic mirror and focused through a $f = 500$ mm lens into the extraction region of a linear time-of-flight mass spectrometer (TOF-MS) housed in a conventional two-chamber differentially pumped molecular beam apparatus. Fs mass-selected transients were obtained by monitoring the ion intensities of specific mass channels with a boxcar integrator while the pump vs. probe delay time was scanned. For all transients presented here the angle between the pump- and probe-laser polarizations was set at the magic angle (54.7°) to minimize the rotational coherence effect.

3. Results and discussions

Fig. 1 shows the transients obtained by monitoring the parent, acetyl intermediate, and methyl product ion signal as a function of pump–probe delay time for the photodissociation of acetone-h_6 and acetone-d_6 at 195 and 194.5 nm, respectively. These transients encompass the entire dynamics of the reaction: the initial state decay (parent), intermediate evolution (acetyl), and the products formation (methyl). Intuitive comparisons of these results immediately suggest that acetone-d_6 exhibits a slower dynamics than its undeuterated counterpart in every stage of the reaction. In the followings, we will discuss the isotope effect in each case and their implications to the dissociation dynamics.

3.1. The parent transients

As shown in Fig. 1A inset, the acetone-h_6 parent transient decays exponentially with a time constant of 4.2 ps, whereas the acetone-d_6 parent transient decays with a much longer time constant of 13.8 ps. These transients and time constants are very similar to those reported previously by other groups [12,13], and indicate that the initial-state dynamics near the acetone S_2 zero-point region slows down by a factor of about three upon deuteration. This relatively large isotope effect suggests that the promoting modes in the $S_2 \rightarrow S_1$ IC may involve C–H stretches and/or CH_3 torsion. The relatively slow $S_2 \rightarrow S_1$ IC of 4.2 ps in acetone-h_6 has been attributed to the extremely large S_2–S_1 energy gap of 2.6 eV [22]. In acetone-d_6 the higher quantum numbers in these modes at S_1 levels isoenergetic to the initial state

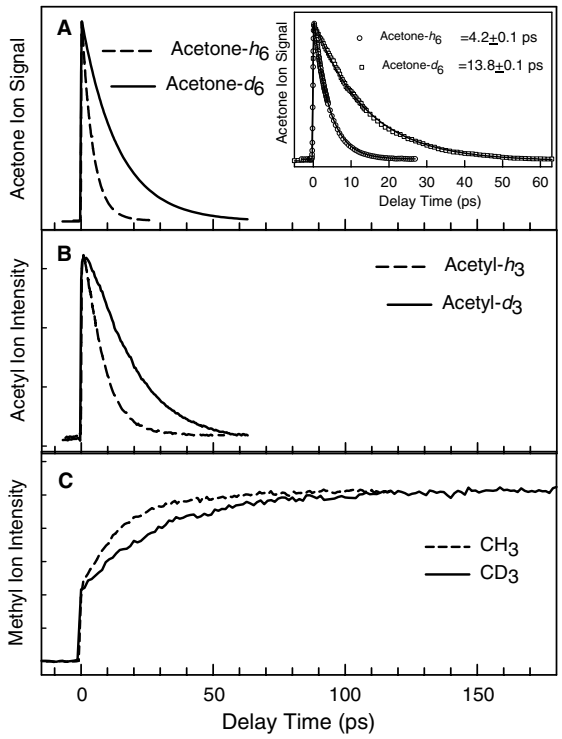

Fig. 1. Mass-selected pump–probe multiphoton ionization transients obtained by monitoring (A) parent-ion, (B) acetyl-ion, and (C) methyl-ion intensities for photodissociation of acetone-h_6 (dashed traces) and acetone-d_6 (solid traces) at 195 and 194.5 nm, respectively. All transients are plotted in the same time scale for easy comparison. The inset in (A) shows the best fits (solid lines) to the acetone-h_6 (open circles) and acetone-d_6 (squares) parent transients with a single-exponential decay convoluted with a Gaussian response function of 270 fs (FWHM).

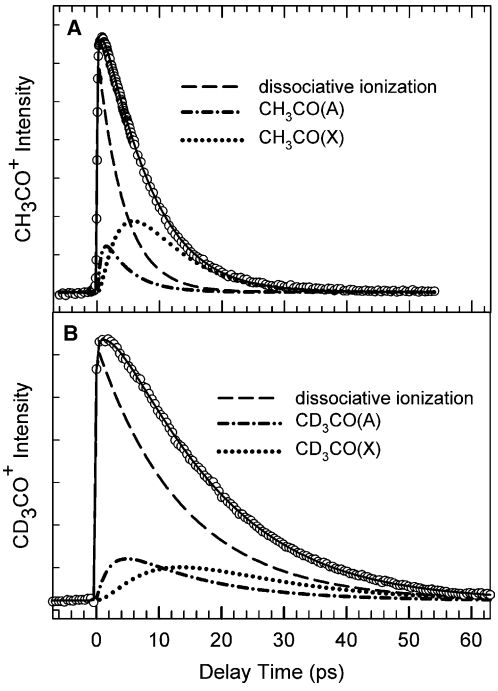

Fig. 2. Best fits of the S_1D kinetic model Scheme 1 to the acetyl-h_3 (A) and acetyl-d_3 (B) transients. Open circles are the experimental data points and the solid lines are the results of the best fits. The dashed, dash-dotted, and dotted lines represent the decomposed contributions from the initial-state dissociative ionization, acetyl ($\tilde{A}$) and acetyl ($\tilde{X}$) components, respectively, as also indicated in the figures.

can further decrease the Franck–Condon overlaps, and hence slow down the internal conversion. This is similar to the 2-D description used to explain the pronounced isotope effect observed in the predissociation of CD_3I Rydberg state [25]. It is also interesting to note that nearly the same effect had been observed for the acetone lifetimes at the S_1 zero-point level: ~1 μs for acetone-h_6 and 3.2 μs for acetone-d_6 [2]. The decay of the acetone S_1 zero-point level has been shown to be mainly due to IC to the S_0 state [4]. The similar isotope effects observed for $S_2 \rightarrow S_1$ and $S_1 \rightarrow S_0$ IC are probably not surprising, because the S_2–S_1 (2.6 eV) and S_1–S_0 (3.8 eV) energy gaps are similarly large.

3.2. The acetyl-intermediate transients

The acetyl-h_3 and acetyl-d_3 transients are shown in Fig. 1B and Fig. 2. The instantaneous rises in both cases are due to the dissociative ionization of the initial state, as has been discussed in our previous reports [22,23]. Both transients were fitted to the S_1D kinetic model shown in Scheme 1. The fits included components for the initial-state dissociative ionization, $CH_3CO(\tilde{A})$ and $CH_3CO(\tilde{X})$ [22,23]. As discussed elsewhere [22], the internally converted hot S_1 state is not expected to be ionized due to the extremely large S_2–S_1 energy gap of 250 kJ/mol (2.6 eV) and is therefore not included in the fits. The time constants determined from the acetyl-d_3 transient are: $\tau_{1d} = 13.8 \pm 0.1$ ps (fixed), $\tau_{2d} = 2.3 \pm 0.2$ ps, $\tau_{3d} = 0.1 \pm 0.05$ ps, $\tau_{4d} = 8.6 \pm 0.1$ ps. The time constants determined from the acetyl-h_3 transients have been reported previously ($\tau_1 = 4.2$ ps, $\tau_2 = 0.6$ ps, $\tau_3 = 0.1$ ps, $\tau_4 = 6.2$ ps) [22]. The ultrafast internal conversion from acetyl ($\tilde{A}$) to acetyl ($\tilde{X}$) in both cases (τ_3 and τ_{3d}) is probably due to the near degeneracy of the two states at the linear CCO geometry. Similar time scales have been reported for formyl radical (HCO) $\tilde{A} \rightarrow \tilde{X}$ conversion through line width measurements [26].

The much longer τ_{2d} indicates that the adiabatic dissociation on the acetone S_1 surface slows down by a factor of about four in acetone-d_6! This large isotope effect is not surprising, because a much higher density of states due to the lower vibrational frequencies in acetone-d_6 is expected to slow down the adiabatic dissociation over a similar barrier height on the S_1 surface. The fitting of the acetyl-d_3 transient revealed an apparent decay of 8.6 ps for $CD_3CO(\tilde{X})$, which is also slower than its counterpart in the acetyl-h_3 case (6.2 ps) [22]. We have shown in our previous reports [22] that this apparent decay does not reflect the true dynamics of the secondary dissociation and attributed it to a combination of dissociation (k_4') and CCO bending relaxation (k_4''). Both steps are expected to reduce the acetyl ion signal, and therefore a combined rate constant, $k_4 = k_4' + k_4''$, was used to represent the apparent

decay of acetyl($\tilde{X}$). The CCO bending relaxation (k_4'') decreases the acetyl ionization efficiency due to the unique structural difference between the acetyl ground state and its cation: the equilibrium structure of $CH_3CO(\tilde{X})$ is bent and has an inversion barrier of ~1 eV [15,16], whereas the CH_3CO^+ ion assumes a linear equilibrium geometry. The consequence of this difference is that the vertical ionization potential (IP) of $CH_3CO(\tilde{X})$ at the linear CCO geometry is 5.8 eV, but becomes 8.4 eV at its bent equilibrium position [15,16,22]. Because a rather large fraction of the vibrational energy in $CH_3CO(\tilde{X})$ is expected to be initially localized in the CCO bending mode [22], the highly excited CCO bending motion can facilitate two-photon ionization of $CH_3CO(\tilde{X})$ by the probe laser. When a certain fraction of the CCO bending energy is dissipated into other modes, the vertical IP becomes too high to be reached at the two-photon ionization level. The bend-relaxed acetyl intermediate thus becomes 'dark' (denoted as $CH_3CO(\tilde{X})D$ in Scheme 1), and therefore its decay does not appear in the acetyl transient.

3.3. The methyl-product transients

The transients obtained by monitoring CH_3 and CD_3 mass channels are shown in Fig. 1C and 3. Again, their general appearances are very similar, except that the CD_3 transient rises more slowly. The initial instantaneous rises in both transients are due to dissociative ionization of the initial state and intermediate, as discussed elsewhere [22]. Both transients were fitted to the S_1D mechanism Scheme 1 [22] and the results are shown in Fig. 3. The time constants obtained from fitting the acetone parent and acetyl transients (τ_1, τ_2, τ_3, τ_4) were fixed while all other parameters were varied during the fits. The time constant τ_{5d} determined from the CD_3 transient is 43 ps, which is much longer than its counterpart in the acetone-h_6 case (25 ps) [22]. We have shown in our previous reports that in acetone-h_6 photodissociation the CH_3-product transient contains a component that rises more slowly than the acetyl signal decays [22]. This effect is even more pronounced in acetone-d_6: the 43 ps rise resolved in the CD_3 transient is five times slower than the apparent acetyl decay (8.6 ps) observed in the acetyl-d_3 transient! This suggests that the apparent decay observed in the acetyl transient does not reflect the true dynamics of the secondary dissociation.

The amplitude ratio of primary CD_3 to the secondary CD_3 resolved in the fit is 1:1.1 ± 0.1. Since the quantum yield for three-body dissociation into $2CD_3 + CO$ is close to unity [6,9] and our probe laser detects only the vibrationless methyl fragments, this ratio implies that the extent of vibrational excitation in primary and secondary CD_3 must be very similar. This is in contrast to the acetone-h_6 case in which the primary to secondary CH_3 amplitude ratio of 1:3 suggests a much vibrationally colder secondary methyl [22,23]. Assuming the amplitudes of the dissociative ionization components are similar in CH_3 and CD_3 transients, it can be inferred that the contribution of the primary methyl increases significantly by more than a factor of two in the CD_3 transient. This suggests that the primary CD_3 produced in acetone-d_6 photodissociation is vibrationally colder than primary CH_3 produced in the acetone-h_6 case. In our previous work, we have shown that the umbrella mode is highly excited in primary CH_3 fragments and attributed it to the ultrafast primary dissociation of 0.6 ps and the large structural change along the umbrella mode during the reaction [22]. In the acetone-d_6 case, the primary dissociation on the S_1 surface is much slower (2.4 ps), and therefore it may have more time to dissipate the extra energy in the methyl umbrella motion to other modes of the dissociating complex and thus makes primary CD_3 vibrationally colder.

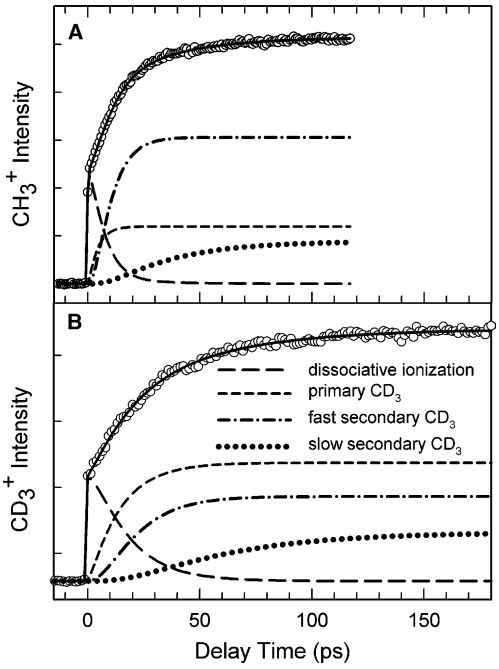

Fig. 3. Best fits of the S_1D kinetic model (Scheme 1) to the CH_3 (A) and CD_3 (B) transients. Open circles are the experimental data points and the solid lines are the results of the best fits. The long-dashed, short-dashed, dash-dotted, and dotted lines represent the decomposed contributions from the dissociative ionization, primary methyl, fast secondary methyl and slow secondary methyl components, respectively, as also indicated in (B).

The very complex dynamics involved in the secondary dissociation of hot acetyl radical has been discussed in our previous report [22,23]. We proposed that the non-uniform initial vibrational distribution and the very slow CCO bending relaxation result in two discernable reaction time scales (see Section 1). According to the fit shown in Fig. 3B, the ratio of the fast to slow secondary CD_3 components is about 1.8. This branching ratio and the apparent acetyl decay of 8.6 ps give $\tau'_{4d} = 13.4$ ps and $\tau''_{4d} = 24$ ps. Comparing these two time constants with their counterparts in the acetone-h_6 case ($\tau'_4 = 8.2$ ps and $\tau''_4 = 25$ ps), one finds that the fast secondary dissociation (k'_4) slows down by a factor of 1.63 (k_h/k_d) in acetyl-d_3. On the other hand, the rate of CCO bending-energy dissipation (k''_4) re-

mains about the same! The latter is consistent with our speculation [22] that the very weak coupling between the CCO bend and other modes hinders the energy flow, i.e., a bottleneck in IVR may exist, and therefore the rate (k_4'') stays nearly unchanged even upon full deuteration.

The slow secondary dissociation (k_{5d}) step in acetyl-d_3 is found to take about 43 ps, giving the CD_3 transient the very slow-rising appearance. Note that, without inclusion of this long component, any kinetic models based on time scales obtained from parent and intermediate transients (<14 ps) cannot satisfactorily describe the slow-rising behavior observed in the CD_3 transient. This step is the dissociation of colder portion of the acetyl ensemble after the concurrent processes of fast secondary dissociation and CCO bending relaxation. In acetyl-h_3 this slow secondary dissociation step (k_5) takes about 25 ps, and therefore there is also a significant isotope effect of $k_h/k_d = 1.72$. Previous results regarding the isotope effect in the secondary dissociation in the title reaction have been controversial in the literatures [12,13]. Here, our methyl-product results clearly indicate that there is a substantial isotope effect ($k_h/k_d = 1.6$–1.7) in the secondary dissociation of the hot acetyl intermediate.

4. Conclusions

In this study, we have compared the photodissociation dynamics of acetone-h_6 and acetone-d_6 S_2 state by examining the temporal evolutions of their initial state, intermediate and the methyl products. All transients obtained for acetone-d_6 can be well described by the same model devised previously for acetone-h_6, giving further supports to the S_1D mechanism. In every stage of the reaction significant 'normal' isotope effects were observed: upon full deuteration the initial-state decay due to S_2 to S_1 IC slows down by a factor of 3; the subsequent adiabatic dissociation on the S_1 surface slows down by a factor of 4; and the secondary dissociation of the acetyl intermediates slows down by a factor of about 1.6. These isotope effects are qualitatively consistent with the S_1D mechanism and provided important insights into the complex dynamics of the reaction.

Acknowledgements

This work was supported by the MOE program for Promoting Academic Excellence of University (89-FA04-AA) and by the National Science Council of Taiwan, R.O.C. (NSC-93-2113-M-007-031).

References

[1] E.K.C. Lee, R.S. Lewis, Adv. Photochem. 12 (1980) 1.
[2] O. Anner, H. Zuckermann, Y. Haas, J. Phys. Chem. 89 (1985) 1336.
[3] M. Baba, H. Shinohara, N. Nishi, N. Hirota, Chem. Phys. 83 (1984) 221.
[4] Y. Haas, Photochem. Photobiol. Sci. 3 (2004) 6.
[5] E.L. Woodbridge, T.R. Fletcher, S.R. Leone, J. Phys. Chem. 92 (1988) 5387.
[6] P.D. Lightfoot, S.P. Kirwan, M.J. Pilling, J. Phys. Chem. 92 (1988) 4938.
[7] L.D. Waits, R.J. Horwitz, J.A. Guest, Chem. Phys. 155 (1991) 149.
[8] K.A. Trentelman, S.H. Kable, D.B. Moss, P.L. Houston, J. Chem. Phys. 91 (1989) 7498.
[9] S.W. North, D.A. Blank, J.D. Gezelter, C.A. Longfellow, Y.T. Lee, J. Chem. Phys. 102 (1995) 4447.
[10] S.K. Kim, S. Pedersen, A.H. Zewail, J. Chem. Phys. 103 (1995) 477.
[11] J.C. Owrutsky, A.P. Baronavski, J. Chem. Phys. 108 (1998) 6652.
[12] J.C. Owrutsky, A.P. Baronavski, J. Chem. Phys. 110 (1999) 11206.
[13] Q. Zhong, L. Poth, A.W. Castleman, J. Chem. Phys. 110 (1999) 192.
[14] E.W.G. Diau, C. Kotting, A.H. Zewail, Chem. Phys. Chem. 2 (2001) 273.
[15] T.I. Solling, E.W.G. Diau, C. Kotting, S. De Feyter, A.H. Zewail, Chem. Phys. Chem. 3 (2002) 79.
[16] E.W.G. Diau, C. Kotting, T.I. Solling, A.H. Zewail, Chem. Phys. Chem. 3 (2002) 57.
[17] E.W.G. Diau, C. Kotting, A.H. Zewail, Chem. Phys. Chem. 2 (2001) 294.
[18] W.K. Chen, J.W. Ho, P.Y. Cheng, Chem. Phys. Lett. 380 (2003) 411.
[19] S.A. Buzza, E.M. Snyder, A.W. Castleman, J. Chem. Phys. 104 (1996) 5040.
[20] G.A. Gaines, D.J. Donaldson, S.J. Strickler, V. Vaida, J. Phys. Chem. 92 (1988) 2762.
[21] H. Zuckermann, B. Schmitz, Y. Haas, J. Phys. Chem. 92 (1988) 4835.
[22] W.K. Chen, J.W. Ho, P.Y. Cheng, J. Phys. Chem. A 109 (2005) 6805.
[23] W.K. Chen, P.Y. Cheng, J. Phys. Chem. A 109 (2005) 6818.
[24] J.W. Hudgens, T.G. DiGiuseppe, M.C. Lin, J. Chem. Phys. 79 (1983) 571.
[25] M.H.M. Janssen, M. Dantus, H. Guo, A.H. Zewail, Chem. Phys. Lett. 214 (1993) 281.
[26] J.C. Loison, S.H. Kable, P.L. Houston, I. Burak, J. Chem. Phys. 94 (1991) 1796.